PHYSICAL REVIEW B VOLUME 26, NUMBER 10 15 NOVEMBER 1982

Symmetric relaxation of the hydrogen-saturated silicon vacancy

Warren E. Pickett
Condensed Matter Physics Branch, Naval Research Laboratory, Washington, D.C. 20375
(Received 9 June 1982)

With the use of the self-consistent pseudopotential method, the Hellman-Feynman theorem is applied to study the symmetric relaxation in the hydrogen-saturated vacancy (HSV) which has been used previously to model the electronic properties of amorphous silicon hydride. The hydrogen and nearest-neighbor silicon atoms are found to relax outward by 0.46 and 0.35 a.u., respectively. The primary effect of this relaxation, which is driven by the large H-H interactions in the ideal HSV, is to *restore* the depleted local H density of states just below the band gap. It is suggested that geometries other than those considered here may lead to more stable configurations.

I. INTRODUCTION

Recently several investigators have used the hydrogen-saturated vacancy (HSV) in Si to model the electronic structure and transport properties of hydrogenated amorphous silicon (a-SiH_x). A tight-binding coherent potential approximation (CPA) treatment[1] on a random 5% "alloy" of HSV's in a silicon lattice displayed a valence-band spectrum very similar to that of a-SiH_x as well as reproducing the experimentally observed widening of the gap when the H content is increased. The self-consistent electronic structure of the HSV itself has been studied from both the supercell[2] and the isolated-defect[3] approaches. Both of these studies found the density of states (DOS) immediately below the gap to be strongly depleted around the H sites, and the former study (Ref. 2, hereafter referred to as I) also found a DOS *increase* around the H sites for conduction states immediately above the gap.

The depletion of conduction-band states near the gap by H has been suggested[3,4] as the cause of the low hole mobility in a-SiH_x, and dc transport calculations[5] on the CPA model[1] have borne out this qualitative picture. More recently, a calculation[6] of the absorption coefficient (i.e., ac conductivity) based on the CPA model has suggested an interpretation of the difference between the "optical gap" and the "DOS gap" in a-SiH_x. Thus it seems that the HSV has provided a reliable basis for understanding several of the crucial properties of a-SiH_x.

The interpretation discussed above has all been based on the electronic structure of the *ideal* HSV. However, in I it was emphasized that the large repulsion between H atoms in the ideal HSV was likely to lead to substantial atomic relaxation in this defect, and a preliminary study of the magnitude of the relaxation has been reported.[7] In this paper we allow the symmetric breathing relaxation of the HSV and find substantial rearrangement of the H local DOS both above and below the gap which must be reconciled with the data on a-SiH_x if the HSV is to remain a viable model for this system.

The plan of the paper is as follows. In Sec. II the numerical procedure which is used to calculate the forces on the atoms is presented. The numerical results and their interpretation are given in Sec. III. The last section is devoted to a discussion of the implications of these results for our current understanding of the electronic properties of a-SiH_x.

II. NUMERICAL TECHNIQUES

The self-consistent pseudopotential (SCP) method has been described in detail elsewhere.[7] The Si and H local pseudopotentials, Hedin-Lundqvist exchange-correlation potential, supercell size corresponding to eight Si atoms, and calculation of local DOS (LDOS) are as described in I. The novel feature of the present work is the calculation of forces on atoms using the Hellman-Feynman (HF) theorem.[8] Formal aspects of the HF theorem in density-functional theory have been discussed elsewhere.[9] However, since this study may be the first of its kind for a model of a localized defect in a

 ©1982 The American Physical Society

bulk solid, and since technical aspects of the calculation of HF forces have not been presented in much detail elsewhere, selected details of the present calculations will be presented in this section.

A. Hellman-Feynman force calculations

For a given atomic configuration $\{\vec{R}_j\}$, the force $\vec{F}_j$ on an ion at $\vec{R}_j$ is given by

$$\vec{F}_j=\vec{F}_j^{\rm ion}+\vec{F}_j^{e} , \quad (1)$$

where $\vec{F}_j^{\rm ion}$ is the direct Coulomb contribution from all other ions,[9] which can be calculated using an Ewald technique,[10] and $\vec{F}_j^{e}$ is the electronic contribution which takes the classical form

$$\vec{F}_j^{e}=\int d^3r\,\rho(r)\vec{\nabla}v_j(r-R_j) \quad (2)$$

in terms of the local ionic pseudopotential v_j. The charge density ρ should be the "exact" charge density, i.e., that which satisfies the local-density-functional equations. An approximate charge density, which might lead to a reasonable total energy $E_{\rm tot}\{\vec{R}_i\}$ (which is variational in ρ) and thereby to reasonable forces from the numerical derivative $\Delta E_{\rm tot}/\Delta\vec{R}_j$, can lead to widly uncontrolled results for $\vec{F}_j$ if the HF expression is applied directly. An example is the Gordon-Kim[11] procedure for deriving the forces between two closed-shell ions from a total charge density approximated by the sum of two spherical ionic densities. Direct application of the HF theorem to this approximate charge density leads to nearly vanishing forces for ionic separations of interest, resulting solely from the exponential tail of one ionic charge overlapping the *nucleus* of the other ion, whereas the Gordon-Kim procedure of calculating $E_{\rm tot}$ in an intermediate step is known to be quite reliable.

Physically, the HF force $\vec{F}_j^{e}$ originates from the distortion (dipolar with respect to $\vec{R}_j$) of the valence charge density (away from that of overlapping spherical atomic densities) due to bonding. In practice, the calculated (and therefore approximate) charge density must be (1) converged with respect to $\vec{k}$-point sampling, (2) self-consistent, and (3) represented sufficiently generally to allow the important bonding-charge distortions. A plane-wave representation, either of the total (valence pseudo-) charge density ρ (as done here) or of the distortions of ρ due to bonding, seems to be a particularly satisfactory representation as it is not fixed to particular atomic positions.

For the HSV, $\vec{F}_j^{e}$ was calculated from the expression

$$\vec{F}_j^{e}=i\sum_{G<\bar{G}}\vec{G}v_j(|\vec{G}|)\rho(\vec{G})e^{-i\vec{G}\cdot\vec{R}_j} , \quad (3)$$

where $v_j(G)$ and $\rho(\vec{G})$ are Fourier coefficients of v_j and ρ. The summation limit $\bar{G}$ must be extended until convergence is obtained. Figure 1 shows the convergence of $\vec{F}^{e}$ for both H and Si as $\bar{G}$ is increased. The important contributions to $\vec{F}^{e}$ arise from wavelengths $(2\pi/G)>a_0/4$, where $a_0=10.263$ a.u. is the Si lattice constant. For all results quoted here the cutoff was taken as $\bar{G}^2=27(2\pi/a_0)^2=10$ Ry.

Accurate values of $\vec{F}_j^{e}$ require a charge density which is more accurate than is necessary for simply determining a self-consistent potential or the total energy. This in turn requires more precise eigenvectors of the Hamiltonian matrix $H_{\vec{G}\vec{G}'}$. A common procedure[7] in the SCP method for obtaining eigenvalues efficiently is to construct $H_{\vec{G}\vec{G}'}$ matrix elements up to a large cutoff $G_2^2=E_2$ and use the Lowdin procedure[12] to fold down the eigenvalue problem to a smaller one corresponding to $G_1^2=E_1$. For the present calculations the Lowdin unfolding procedure[12] for subsequently obtaining the eigenvector components up to $G=G_2$ has also been employed. These procedures, which are reminiscent of second-order perturbation theory in the matrix elements $H_{\vec{G}\vec{G}'}$ for $E_1<G^2$, $G'^2\le E_2$, produce eigenvectors of sufficient accuracy for the present purposes. The cutoffs $E_1=4.5$ Ry, $E_2=8$ Ry corre-

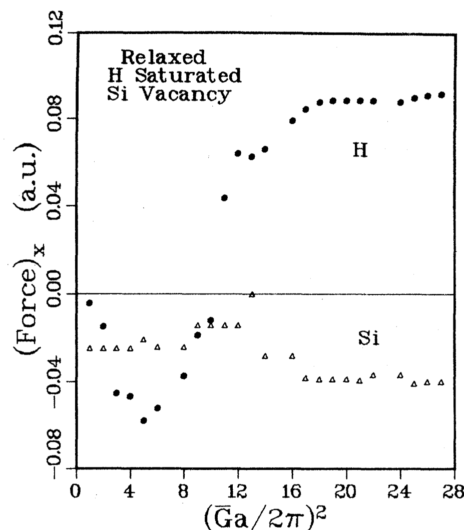

FIG. 1. x component of the electronic contribution to the force, in hartrees/bohr, on H and nearest-neighbor Si atoms, illustrating convergence vs $\vec{G}$-space cutoff $\bar{G}$. Results are for configuration 1.

spond to plane-wave basis sets of approximately 175 and 400 plane waves, respectively, and provide only slightly less accurate solutions to the 400×400 secular equation at substantially less cost than by direct methods.

In Table I examples of the changes in the calculated forces due to large-G components of the wave function are displayed. For this convergence check the single special $\vec{k}$ point[13] was used to approximate the charge density for the ideal configuration, and the Lowdin unfolding procedure was applied to give initially 300 and then 400 plane-wave coefficients of the wave functions. The calculated forces on the H and Si atoms increased in magnitude by 35% and 6%, respectively, while the total energy per atom changed only from -5.5028 to -5.5058 Ry.

The set of four special $\vec{k}$ points[13] for the simple cubic lattice has proven adequate for the HSV supercell for determining ρ. One special point is clearly insufficient, while results almost identical to those from the four-special-point mesh were obtained using the 10- and 35-point regular meshes and the 20-special-point set.

B. Geometry

The HSV supercell is a cube corresponding to the crystalline Si cubic cell of edge length a_0 and containing eight Si sites. For the HSV the Si atom at the origin is replaced by hydrogens at (u,u,u) and equivalent positions tetrahedrally placed around the origin. For the *ideal* HSV, u was chosen[2] as $0.0883a_0$, corresponding to a H$-$Si bond length of Si_3-SiH suggested by Lucovsky.[14] Only symmetric "breathing-mode" relaxations, i.e., atoms relaxing radially from the center of the defect only, of the HSV have been considered. Thus only u and the

TABLE I. Comparison of the x component of the calculated electronic forces (in arbitrary units) on H and Si atoms when 300 or 400 plane-wave coefficients are included in the plane-wave expansion. Contributions from each star of reciprocal-lattice vectors as well as the total are given. Owing to the symmetric placement of the Si atom [at $(a_0/4,a_0/4,a_0/4)$] within the unit cell, several stars G give vanishing contributions to the force independently of $\rho(\vec{G})$.

$\left(\frac{a}{2\pi}\right)\vec{G}$	H 300	H 400	Si 300	Si 400
100	-1.57	-1.60	-9.54	-9.70
110	-3.52	-3.56		
111	-8.78	-8.78		
200	-1.21	-1.23		
210	-4.69	-4.76	1.64	1.66
211	-1.49	-1.48	-0.59	-0.61
220	2.85	3.13		
221	1.61	1.71	1.71	1.75
310	0.32	0.31		
311	11.86	12.66		
222	4.52	4.68		
320	-0.56	-0.63	2.68	3.03
321	0.69	0.77	-4.68	-5.26
400	2.52	2.91		
322	1.42	1.58	-1.54	-1.73
330	0.39	0.44	-0.33	-0.43
331	0.19	0.18		
420	-0.01	-0.02		
421	-0.01	-0.01	-0.05	-0.07
332	0.06	0.07	0.61	0.69
422	-0.04	-0.05		
430	0.21	0.27	-0.58	-0.75
431	0.19	0.24	0.25	0.38
333	0.06	0.07		
Total	5.01	6.90	-10.42	-11.04

coordinate v of the neighboring Si atom at (v,v,v) and symmetric positions are allowed to vary ($v=0.25a_0$ for the ideal HSV). Changes in unit-cell volume have not been considered.

III. RESULTS

A. Relaxation of the HSV

In addition to the ideal HSV geometry, three relaxed geometries have been studied. Their coordinates and the calculated atomic forces are presented in Table II. Configuration 3 was determined from the previous configurations (0,1,2) by fitting forces determined from the harmonic potential-energy expression, valid for small enough displacements,

$$V(u,v)=Au+Bv+Cu^2+Dv^2+Euv\ , \quad (3)$$

to the six calculated forces, and then determining the equilibrium values of u and v. After calculating the forces for configuration 3 (Table II), forces derived from expression (3) were least-squares-fitted twice, to the calculated forces for all four configurations, and separately to configurations 1, 2, and 3 (those nearest equilibrium). From these two potential functions the equilibrium values u_0 and v_0 and their uncertainties (arising from which fit one chooses to use) were found and are given in Table II.

The results of the geometrical relaxation can be summarized as follows. The H atoms relax outward by $\sqrt{3}\,|u_0-u(0)|=0.46$ a.u. [$u(0)=u$ for configuration 0] while the neighboring Si atoms relax outward by 0.35 a.u., resulting in a 7% decrease of the H—Si bond length. This relaxation rotates the Si—Si bond by 4.5° and compresses it by 2.5%. The ideal and relaxed geometries in the (110) plane are shown in Fig. 2. In terms of $\bar{u}=u-u_0$,

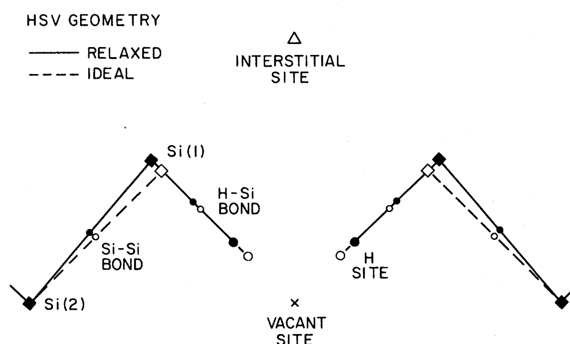

FIG. 2. Schematic geometry of the HSV relaxation in the (110) plane of the supercell. Dashed lines represent the configuration before relaxation.

$\bar{v}=v-v_0$, the potential energy V for small displacements can be written

$$V(\bar{u},\bar{v})=a\bar{u}^2+b\bar{v}^2+c\bar{u}\ \bar{v}\ . \quad (4)$$

From this expression the energy ΔE gained by relaxation is found to be about 1 eV/supercell, i.e., per HSV defect. Direct calculation of ΔE (discussed more fully below) between configurations 0 and 3 is 1.1 eV.

B. Changes in eigenstates and LDOS

As expected, this rather large atomic relaxation leads to significant changes in the hydrogen-related states and LDOS. In Fig. 3 the supercell band structure along Γ-R is shown for both the ideal and relaxed HSV. The states of particular interest in following the effect of relaxation are numbered 1 through 6, and the charges of each of these states within spheres distributed throughout the cell are given in Table III. States 1—3 lie in the lower valence bands and before relaxation each is strongly

TABLE II. x components of H,u and Si,v positions (in units of the lattice constant 10.263 a.u.), and the x components of ionic, electronic, and total forces on H and Si atoms (hartree/bohr). Equilibrium positions are calculated by fitting to quadratic potentials as described in the text; uncertainties (in parentheses) are due to the two separate fits to the calculated forces and *do not include* uncertainties in the calculated forces.

				H			Si	
Configuration	u	v	$F_x^{\rm ion}$	F_x^e	$F_x^{\rm tot}$	$F_x^{\rm ion}$	F_x^e	$F_x^{\rm tot}$
0	0.0883	0.2500	−0.019	0.038	0.019	0.060	−0.041	0.019
1	0.0960	0.2500	−0.090	0.091	−0.001	0.080	−0.040	0.040
2	0.1000	0.2560	−0.108	0.115	0.007	0.036	−0.014	0.022
3	0.1203	0.2730	−0.213	0.202	−0.011	−0.049	0.052	0.003
Equilibrium	0.1142(3)	0.2696(1)	−0.179	0.179[a]	0.0	−0.040	0.040[a]	0.0

[a]Calculated from equilibrium condition $F_x^{\rm tot}=0$.

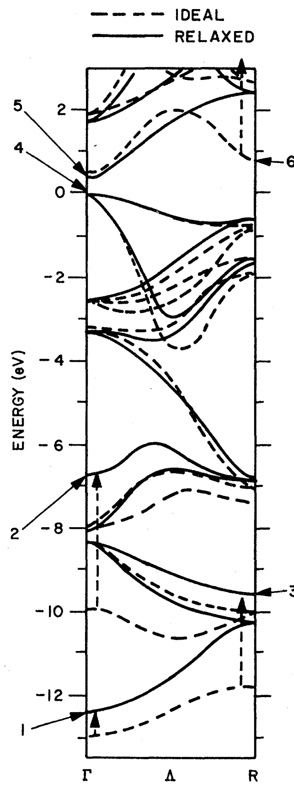

FIG. 3. Supercell band structure along the Γ-R direction for configuration 0 (ideal) and configuration 3 (near equilibrium). Dotted arrows indicate states which are affected strongly by the relaxation. Numbers label states discussed in text and referred to in Table III.

localized near the H atoms. The outward relaxation of the H atoms decreases the overlap of the attractive H pseudopotentials in this region. As a result these states rise in energy and lower their amplitude near the H atoms, although state 2 (and to a lesser extent state 3) remains strongly H related.

States 4—6 lie near the gap and therefore are crucial in determining low-excitation-energy properties. State 4 is the uppermost valence band whose eigenvalue is used to fix the energy zero in Figs. 3 and 4. [With respect to the average potential $V_{\text{tot}}(\vec{G}=\vec{0})$, the energy of state 4 moved downward by 0.5 eV during relaxation.] From Table III it can be seen that for this state the charge near H nearly doubles during relaxation. Conversely, the charge on the lower-conduction-band state 5 decreases dramatically near and between the H atoms during relaxation, although its eigenvalue changes very little. Finally, state 6, the low-conduction-band state at R in the ideal HSV, is raised by nearly 3 eV by the relaxation although its strong H-related character is not changed dramatically (Table III). Both states 5 and 6 have large amplitudes in the interstitial regions of the cell.

The LDOS's for the spheres along the bonding chain pictured in Fig. 2 are given in Fig. 4 along with the total DOS. The only notable change in the total DOS occurs at the bottom of the valence bands, where the strongly H-related peak at −13 to −12 eV found in I for the ideal HSV is found to merge with the low Si valence states during relaxa-

TABLE III. Relative charges within each of the equal-volume spheres at the positions indicated in Fig. 2 for the six states designated in Fig. 3. Both ideal (configuration 0, in parentheses) and near equilibrium (configuration 3) values are given, with normalization such that a uniform state will have a value 1.00 within each sphere. Also given below is the total charge (in electrons) within each sphere and the ratio "charge (relaxed)/charge (ideal)."

State number	Vacant site	H	H−Si bond	Si(1)	Si−Si bond	Si(2)	Interstitial
1	0.44	1.13	1.53	1.61	2.15	1.74	0.61
	(7.90)	(5.29)	(2.72)	(1.66)	(1.06)	(1.06)	(0.14)
2	6.27	7.92	4.60	0.73	0.50	0.60	0.82
	(13.15)	(7.35)	(1.55)	(0.54)	(1.68)	(1.15)	(0.26)
3	1.49	3.06	3.20	2.45	1.75	0.38	1.15
	(17.46)	(11.00)	(4.25)	(1.29)	(0.05)	(0.25)	(0.05)
4	0.66	2.86	2.20	1.36	2.75	1.21	0.05
	(0.83)	(1.50)	(1.52)	(1.21)	(1.40)	(2.74)	(0.07)
5	1.98	1.10	0.31	0.63	0.89	1.37	8.22
	(5.27)	(2.18)	(0.90)	(0.77)	(0.09)	(0.54)	(4.99)
6	8.64	2.96	1.61	1.80	1.12	0.15	4.59
	(8.58)	(3.61)	(2.13)	(2.34)	(0.18)	(0.71)	(1.57)
Total charge	0.84	2.35	2.21	1.39	1.34	2.03	0.32
	(2.10)	(2.12)	(1.90)	(1.51)	(1.79)	(1.47)	(0.20)
Ratio	0.40	1.11	1.17	0.92	0.75	1.38	1.63

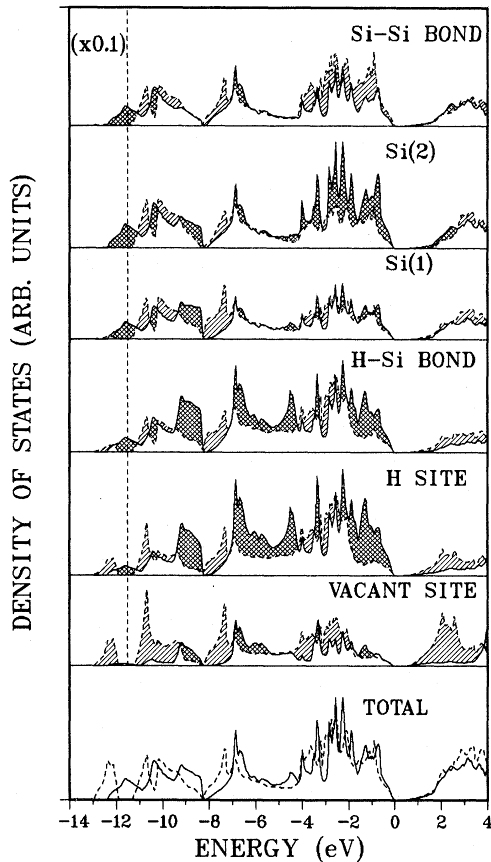

FIG. 4. Total and local densities of states in the spherical regions pictured in Fig. 2. In the LDOS curves the dashed peak below -12 eV has been divided by ten. All LDOS are plotted on the same scale. States move from the single- to the double-cross-hatched regions during relaxation.

tion. Accordingly, the vacant-site and H-site LDOS's show a general decrease in the -13- to -9-eV region.

There is a large *increase* in the LDOS just below the gap at the H site, H—Si bond, and the second-neighbor Si ["Si(2)"], of which the latter may be a "supercell effect" which indicates that for these energies the charge perturbation extends to larger distances. Conversely, near the bottom of the conduction bands there is a strong *decrease* in the LDOS at the vacant site, H site, and H—Si bond, together with a significant increase near Si(2) which again may be a supercell effect.

It should be noted that little can be learned about the energetics of the relaxation solely from the DOS, i.e., from the sum over occupied states of the eigenvalues. It is found that the change in eigenvalue [relative to $V_{\text{Hartree}}(\vec{G}=\vec{0})=0$] sum between configurations 3 and 0 is -7.70 eV, while the change in the Coulomb double-counting correction[9] is a similar contribution of -7.24 eV. The Ewald and exchange-correlation correction energy differences are 13.10 and 0.72 eV, giving the final energy change (gain) from relaxation of -1.12 eV. Thus the eigenvalue sum contribution has the same sign as the total energy difference in this case, but other contributions compete in importance with the eigenvalue sum.

C. Charge density

The overall appearance of the charge density of the relaxed HSV in the (110) plane is similar to that of the ideal HSV in I and is not shown. The difference plot in Fig. 5 of ρ(configuration 3)$-\rho$(ideal) indicates that the charge distortion accompanying atomic relaxation is dominated by a removal of charge from between the tetrahedron of H atoms and the addition of charge to Si—H bonding region. This rearrangement of charge can be accounted for qualitatively by the rigid motion of atomiclike H and Si charge densities. In addition, there is an increase in charge in the H—Si backbonding position (more than 1 a.u. from the Si nucleus) which is consistent with this rigid-atom picture. The increase in charge in the Si—Si bond likewise can be ascribed to the 2.5% compression of this bond; its asymmetric form, however, suggests a distortion of the bond charge due to bond rotation. The atomic relaxation also results in a decrease of the already small charge density in the interstitial region.

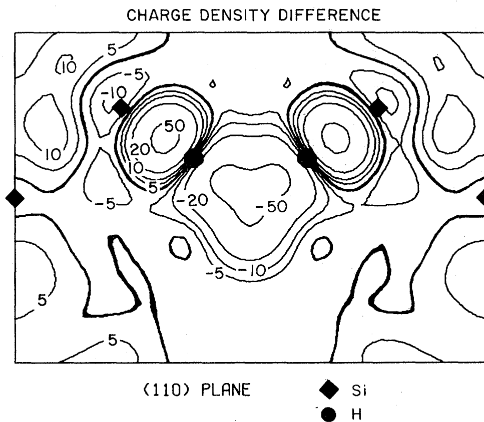

FIG. 5. Plot in the (110) plane of the difference in charge density between configuration 3 and configuration 0; i.e., "relaxed" minus "ideal." Contours are drawn at 0 (heavy contour), ± 5, ± 10, ± 20, and ± 50 electrons/cell.

IV. DISCUSSION

The preceding section has described the symmetric, constant volume relaxation of H and neighboring Si atoms in the HSV. The restriction to constant volume has compressed the H–Si and Si–Si bonds by 7% and 2.5% compared to their "equilibrium" values, indicating the "relaxed" HSV as described here is under pressure. The compressibility of crystalline silicon and the Si–Si bond compression (corresponding to $\Delta V/V = 7.5\%$) implies a local pressure of the order of 75 kbar. A full relaxation of the HSV (within the breathing-mode constraint assumed here) would require minimizing the energy with respect to lattice constant, then again allowing internal atomic relaxation, and iterating this procedure to convergence. It is not clear that the result of such a calculation would justify the expense, so "full relaxation" in this sense has not been attempted.

As a first approximation the "fully relaxed" HSV (in the sense described above) can be approximated by the present relaxed atomic configuration, but with lattice constant expanded by 2.5% to restore the Si–Si bond to its length in crystalline silicon. This leaves the H–Si bond compressed by 4.5% by the H-H interactions.

One important property which can be sensitive to the variation of lattice constant and to internal stresses is the vibrational frequency of the system. From the potential-energy expression (4) and atomic masses the breathing-mode frequencies are found to be 3300 and 425 cm^{-1} for "optic" and "acoustic" modes, respectively. [These modes however are not normal modes of the present supercell lattice since the Si(2) atoms are fixed.] The high-frequency H-Si stretching mode is 50% above the 2100-cm^{-1} band assigned to H-Si stretching modes[14–16] in a-SiH_x. Volume relaxation would lower the calculated frequency, perhaps drastically, considering the large but canceling electronic and ionic forces on H (Table II) at equilibrium.

Experience in electronic structure calculations indicates, however, that the qualitative features of the electronic structure of the HSV should not vary significantly with a 2.5% increase in lattice constant. Thus the changes in the LDOS near the gap should be taken seriously and their implications given consideration.

Brodsky[4] has suggested a "quantum-well model" for a-SiH_x in which it is assumed that H–Si bonds deplete the valence-band DOS's near the gap and result in localization of the wave functions within 0.6 eV of the valence-band edge. Support for this model arose from the isolated HSV calculations of DiVincenzo *et al.*[3] (and also from I), and the model could explain qualitatively certain optical and transport processes. On the contrary, the present study shows that most of the H–Si bonding states are restored to the region $-0.6 < E < 0$ eV by symmetric relaxation.

The CPA HSV alloy model of Papaconstantopoulos and Economou[1] (PE) also indicates a strong depletion of valence-band states just below the gap. Moreover, this model explains in *a quantitative manner* a number of properties of a-SiH_x: (1) removal of states from, and the widening of, the gap upon hydrogenation,[1] (2) existence of Si–H antibonding resonance states[1,5] just *above* the gap, (3) the absorption coefficient[6] in the range $2 < h\nu \leq 3$ eV, and (4) the position of H-related bonding states in the valence band.[1] From the "H-site" and "H–Si bond" LDOS in Fig. 4 it is clear that *symmetric breathing relaxation of the HSV removes precisely those features of the H-related LDOS in the CPA model which are responsible for giving an interpretation of properties (1)–(3) above.* Property (4)—the position of H-related photoemission peaks—is less sensitive to the relaxation calculated here, with relaxation causing peaks to shift away somewhat from those measured by von Roedern *et al.*[17] but more toward agreement with those found by Smith and Strongin.[18]

As a consequence, it appears that the ideal HSV provides a good model of a local defect upon which an alloy model of a-SiH_x can be built, while our relaxed HSV fails. This result, in itself, implies no contradiction, as PE have emphasized that it is the local H-Si chemical environment rather than the geometrical arrangement of the cluster of four H atoms which is the determining factor in their model.

This result may however be interpreted as suggesting only that the present model of relaxed HSV does not actually occur, but rather is dynamically unstable towards a lower-symmetry, lower-energy configuration. The present study guarantees only that the relaxed configuration is stable with respect to breathing-type distortions with full tetrahedral symmetry, and that it is not Jahn-Teller unstable toward a lower-symmetry configuration. However, the restricted minimum-energy configuration found here may well be a saddle point in the full configuration space of atomic distortions.

In such a case the H (and Si) atoms are dynamically unstable with respect to motion perpendicular

to the (111) H—Si bonding directions. The fully relaxed configuration could be a low-symmetry one which allows lengthening of the compressed H—Si and Si—Si bonds toward more typical lengths as well as the avoidance of strong H-H interactions, at the cost of relatively low-energy distortions of H—Si—Si and Si—Si—Si bond angles. Avoiding the compression of the H—Si bond should leave the H LDOS depleted in the upper valence-band region, similar to that of the ideal HSV in I, and therefore retain the single feature (the local H-Si chemical environment discussed by PE) most essential to modeling a-SiH_x.

Assuming a complete loss of symmetry, the configuration space consists of the coordinates of each of the four H and four Si atoms, a total of 24 variables. The present approach of calculating *forces* rather than energies provides the only reasonable approach to finding the lowest-energy configuration in such a case. However, the loss of symmetry leads to a large increase in computational effort (from $\vec{k}$-point sampling), and nothing is known at present about the number of configurational iterations to be expected to reach equilibrium in such a large parameter space. Nevertheless restricted relaxations along these lines may be studied in the near future.

ACKNOWLEDGMENTS

I have benefitted from numerous discussions with D. A. Papaconstantopoulos, E. N. Economou, B. M. Klein, L. L. Boyer, and C. S. Wang on various aspects of this work and from comments on the manuscript. Useful computer codes were made available by J. Ihm and B. Chakraborty. The technical assistance of A. Koppenhaver is gratefully acknowledged. This work was supported in part by the Solar Energy Research Institute through an interagency agreement between the Naval Research Laboratory and the Department of Energy, and by the Office of Naval Research under Contract No. N00014-79-WR-90028.

[1]D. A. Papaconstantopoulos and E. N. Economou, Phys. Rev. B 24, 7233 (1981).

[2]W. E. Pickett, Phys. Rev. B 23, 6603 (1981).

[3]D. P. DiVincenzo, J. Bernholc, M. H. Brodsky, N. O. Lipari, and S. T. Pantelides, in *Tetrahedrally Bonded Amorphous Semiconductors (Carefree, Arizona),* A Topical Conference on Tetrahedrally Bonded Amorphous Semiconductors, AIP Conf. Proc. No. 73, edited by R. A. Street, D. K. Biegelsen, and J. C. Knights (AIP, New York, 1981), p. 156.

[4]M. H. Brodsky, Solid State Commun. 36, 55 (1980).

[5]W. E. Pickett, D. A. Papaconstantopoulos, and E. N. Economou, J. Phys. (Paris) Colloq. C4 42, 769 (1981).

[6]W. E. Pickett, D. A. Papaconstantopoulos, and E. N. Economou (unpublished).

[7]J. R. Chelikowsky and M. L. Cohen, Phys. Rev. B 13, 826 (1976).

[8]W. Pauli, *Handbuch der Physik,* 2nd ed. (Springer, Berlin, 1933), Vol. 24, p. 162; H. Hellman, *Einfuhrung in die Quantenchemie* (Deuticke, Leipzig, 1937); R. P. Feynman, Phys. Rev. 56, 340 (1939).

[9]J. Ihm, A. Zunger, and M. L. Cohen, J. Phys. C 12, 4409 (1979).

[10]Codes for calculating F_j^{ion} were kindly provided by J. Ihm.

[11]R. G. Gordon and Y. S. Kim, J. Chem. Phys. 56, 3122 (1972).

[12]P. O. Lowdin, J. Chem. Phys. 19, 1396 (1951).

[13]D. J. Chadi and M. L. Cohen, Phys. Rev. B 8, 5747 (1973).

[14]G. Lucovsky, Solid State Commun. 29, 571 (1979).

[15]W. Paul, Solid State Commun. 34, 283 (1980).

[16]P. John, I. M. Odeh, and M. J. K. Thomas, Solid State Commun. 41, 341 (1982), and references therein.

[17]B. von Roedern, L. Ley, and M. Cardona, Phys. Rev. Lett. 39, 1576 (1977); B. von Roedern, L. Ley, M. Cardona, and F. W. Smith, Philos. Mag. B 40, 433 (1970).

[18]R. J. Smith and M. Strongin, Phys. Rev. B 24, 5863 (1981).